(NASA-CR-136764) OUTER PLANET MISSION GUIDANCE AND NAVIGATION FOR SPINNING SPACECRAFT (Jet Propulsion Lab.) 38 p HC $3.75 CSCL 22A G3/13

N75-17396

Unclas 12957

OUTER PLANET MISSION GUIDANCE AND NAVIGATION FOR SPINNING SPACECRAFT

By

Charles K. Paul
Robert K. Russell
Jordan Ellis

April 26, 1974

Backup Document for AIAA Synoptic Scheduled for Publication in the Journal of Spacecraft and Rockets, June 1975

Jet Propulsion Laboratory
California Institute of Technology
4800 Oak Grove Drive
Pasadena, California 91103

SYNOPTIC BACKUP DOCUMENT

This document is made publicly available through the NASA scientific and technical information system as a service to readers of the corresponding "Synoptic" which is scheduled for publication in the following (checked) technical journal of the American Institute of Aeronautics and Astronautics.

- ☐ AIAA Journal
- ☐ Journal of Aircraft
- ☒ Journal of Spacecraft & Rockets, June 1975
- ☐ Journal of Hydronautics

A Synoptic is a brief journal article that presents the key results of an investigation in text, tabular, and graphical form. It is neither a long abstract nor a condensation of a full length paper, but is written by the authors with the specific purpose of presenting essential information in an easily assimilated manner. It is editorially and technically reviewed for publication just as is any manuscript submission. The author must, however, also submit a full backup paper to aid the editors and reviewers in their evaluation of the synoptic. The backup paper, which may be an original manuscript or a research report, is not required to conform to AIAA manuscript rules.

For the benefit of readers of the Synoptic who may wish to refer to this backup document, it is made available in this microfiche (or facsimile) form without editorial or makeup changes.

OUTER PLANET MISSION GUIDANCE AND NAVIGATION FOR SPINNING SPACECRAFT[†]

Charles Kendall Paul*

Robert Kent Russell*

Jordan Ellis**

Jet Propulsion Laboratory

Pasadena, California

Abstract

The orbit determination accuracies, maneuver results, and navigation system specification for three spinning Pioneer planetary probe missions are analyzed to aid in determining the feasibility of deploying probes into the atmospheres of the outer planets. Radio-only navigation suffices for a direct Saturn mission and the Jupiter flyby of a Jupiter/Uranus mission. Saturn ephemeris errors (1000 km) plus rigid entry constraints at Uranus result in very high velocity requirements (140 m/sec) on the final legs of the Saturn/Uranus and Jupiter/Uranus missions if Earth-based tracking only is employed. The capabilities of a conceptual V-slit sensor are assessed to supplement radio tracking by star/satellite observations. By processing the optical measurements with a batch filter, entry conditions at Uranus can be controlled to acceptable mission-defined levels ($\pm 3^\circ$) and the Saturn-Uranus leg velocity requirements can be reduced by a factor of 6 (from 139 to 23 m/sec) if nominal specified accuracies of the sensor can be realized.

[†]This research was sponsored by NASA Contract NAS 7-100 and conducted at the Jet Propulsion Laboratory, California Institute of Technology, Pasadena, California.

*Senior Research Engineer

**Member of the Technical Staff

Glossary

B	probe miss distance in planetary radii
C_3	twice the injection kinetic energy per unit mass
R	radius at separation in planetary radii
r_p	bus/probe periapsis radius in planetary radii
RA	right ascension of V_∞ vector
T	time before probe vacuum periapsis, in hours
V_∞	hyperbolic excess velocity in km/sec
δ	declination of V_∞ vector
ΔV (along)	separation velocity component along Earth-line, m/sec
ΔV (normal)	separation velocity component normal to Earth-line, m/sec
γ_e	entry flight path angle in degrees
θ_{aim}	B-plane aim angle in degrees

Methodology and Approach

The Missions

The missions analyzed in this study are: (1) a 1979 direct Saturn, (2) a 1980 Saturn/Uranus, and (3) a 1980 Jupiter/Uranus. Table 1 lists the specific nominal trajectory characteristics of the missions. In general, all three missions can be characterized by: (1) high launch energies ($C_3 \approx 130$ km^2/sec^2), (2) spacecraft launch mass of 475 kg, (3) spinning Pioneer-type spacecraft consisting of a bus and a probe for planetary entry, and (4) Titan IIIE/Centaur/TE-364-4 launch vehicle.

The planetary entry aiming strategy is the deflected bus mode in which the probe/bus configuration is aimed for planetary entry and a velocity impulse (on the order of 100 m/sec) is imparted to the bus at several hundred planetary radii before probe entry to target the bus for a planetary flyby. The

bus serves as a communications link between Earth tracking stations and the probe as the probe descends into the planetary atmosphere measuring indigenous environmental elements. (Ref. 1)

Navigation

Navigation problems which plague inner planet missions also exist for outer planet missions, although many of these problems such as poor solar radiation pressure modeling are insignificant compared to spacecraft state perturbations mapped over large distances. For example, errors in modeling the very small time-varying attitude control leakages on board the spacecraft may lead to a corruption of the filtered state estimate which becomes greater as mission duration increases. In addition, errors in the locations of the Earth-based tracking stations, although small, contribute errors to the state estimate which vary directly as the distance to the Earth. The problem of low declination trajectories can affect all classes of planetary missions using conventional radio range and range-rate data. It is more severe for the outer planets since the declination rate is so much lower and if the spacecraft is already in a low declination, it tends to stay there for a long time. To round out this picture, the planet ephemeris and mass errors are far more significant on the distant outer planet missions. Essential to precise planetary navigation involving flybys and entry probes, of course, is the knowledge of the planet's position and its mass.

To provide precise navigation capability for an outer-planet mission with its attendant difficulties, appropriate data types must be used so as to minimize the effect of the above error sources. Ondrasik and Rourke have shown (Ref. 2) that differenced, near-simultaneous range and range-rate data, (QVLBI), when used in conjunction with deweighted, conventional range and

range-rate data, can be of great utility in resolving the difficulties of both low-declination and process noise (attitude control forces). The reason for deweighting of the conventional range and range rate data is the high sensitivity of these data types to process noise (unmodelled accelerations).

The assumptions embodied in the radio navigation analysis are:

1. The data types are range (deweighted standard deviation of 10 km noise), range rate (deweighted std. dev. of 100 mm/sec noise), differenced range (std. dev. of 8.4 m noise), and differenced range rate (std. dev. of 2.8 mm/sec. noise).

2. The data rates assumed are one point/min for range rate and one point/6 hr for range. For simultaneous data, the differenced range rate data is assumed taken at 1 point/min where stations overlap. For differenced range data, only two-station overlap is considered for the three DSN (Deep Space Network) stations, with the station cycle repeating every third day.

3. The data are assumed to begin at S - 80 days (80 days before probe periapsis at Saturn) for the direct Saturn mission and at E (Encounter) - 120, E - 90, and E - 60 days for Saturn and Jupiter on the SU and JU missions. The data are assumed to begin at U - 120 days at Uranus for both the SU and JU missions and end at bus/probe separation. The different tracking intervals at Saturn and Jupiter are employed in the analysis so as to examine filter performance with varying data arcs.

4. The data filter is a minimum variance batch filter. The evaluation, however, is performed in a batch-sequential mode with a two-day batch interval. This type of evaluation allows for an examination of the effects of a stochastic (first-order Markov process) consider parameter on the true filter performance.

5. Six spacecraft position components, six planet ephemeris elements, one planet mass, and one constant solar acceleration component are included in the solution state.

6. "Consider" state parameters affecting the estimate but not estimated themselves are nine Earth station locations and one solar stochastic acceleration component.

7. A priori spacecraft solution state errors are assumed to be 10^6 km for the three position components and 1 km/sec for the three velocity components. The planet ephemeris errors are taken as the full 6 × 6 covariance on the Brouwer and Clemence Set III elements. Position error magnitudes are 400 km for Jupiter, 1000 km for Saturn, and 10,000 km for Uranus. Planet mass errors are taken as 2,000, 40,000, and 80,000 km^3/sec^2 for Jupiter, Saturn and Uranus, respectively. The spacecraft constant radial acceleration error due to gas leakage is taken to be 10^{-12} km/sec^2.

8. The a priori consider state errors consist of station location errors and a stochastic radial acceleration. The station location errors are parameterized as "tight" and "loose" levels reflecting the type of calibration available to establish and maintain equivalent station locations. The "tight" spin radius error is 1 m, the longitude error is 2 m, and the height above equator error is 15 m. The corresponding errors for the "loose" calibration are 3, 5, and 15 m, respectively. The correlation factor between station longitudes is 0.9. The stochastic radial acceleration is treated as a first order Markov process with a standard deviation of 10^{-12} km/sec^2, and a correlation time of 5 days.

Radio data types, as necessary and precise as they are, are not particularly effective in resolving the problems posed by the ephemeris errors during planetary approach. Duxbury (Ref. 3) has shown, however, that an on-board optical sensing system, capable of observing outer planet

satellites relative to the celestial sphere, is quite able to reduce the problem of ephemeris errors significantly. As a result, both on-board optical and Earth-based radio (differenced and conventional range and range-rate) data types were employed in this study. Inasmuch as the vehicle is a Pioneer-class spacecraft (i.e., spin-stabilized), the optical system will be of a different type than that used on the Mariner-class (three-axis stabilized) spacecraft, the latter being basically a television imaging system. What is being considered and will be studied here is called a V-slit sensor, depicted schematically in Fig. 1. This concept is being proposed by TRW to provide on-board navigation measurements on a spinning spacecraft. The concept is for the sensor, as it sweeps a 3° field of view with each spacecraft rotation, to observe stars (brighter than magnitude 4.0) and planetary satellites. The sensor acquires satellite images when their visual magnitudes reach 4 and tracking terminates when the target image exceeds 20 arc sec in the sensor field of view. The sensor determines their cone and clock angles relative to the spacecraft spin axis and some arbitrary celestial reference. These data (radio and optical), combined with the equations of motion of the spacecraft and the satellite motion about the primary, provide the capability for precise planet-relative spacecraft navigation.

The satellite brightness acquisition and size termination tracking constraints are indicated in Table 2. Figure 2 represents the spacecraft viewing geometry at Saturn and Uranus at roughly 10^7 km from the planet's center. The spacecraft cone and clock angles are indicated with 180° cone being the negative Earth line (spin axis). Thus, as the spacecraft spins, the 3' slit describes a celestial ring of constant cone angle. At Saturn, five stars of magnitudes 4 or brighter and the natural satellites of Saturn can be measured in 120° of clock angle rotation in a constant 3° cone angle swath

between 144.5° and 147.5°. One of the available stars is Arcturus. At Uranus a wider clock angle swath is required since the angle between the negative Earth line and Uranus satellites is smaller than at Saturn. This results in less sky being scanned at Uranus for a 2π sweep in clock angle. However, it is seen that between cone angles of 164° and 167°, 10 stars of at least magnitude 4 or brighter, plus Uranus satellites, are available for optical measurements. A star plot was not included for Jupiter since ensuing results will discourage the V-slit sensor utilization for Jupiter flyby. The conclusion is that there are sufficient stars within a 3° field of view of both planets' satellites to feasibly implement the V-slit sensor scheme.

The direct Saturn mission was analyzed assuming radio-only navigation whereas the Saturn/Uranus and Jupiter/Uranus mission assumed radio coupled with optical navigation.

Maneuver Strategy

The midcourse velocity correction strategy employs a first correction 5 days after launch to correct the Saturn B-plane miss ellipse due to the Titan IIIE/Centaur/TE-364-4 injection errors. At Earth plus 5 (I + 5) days, orbit determination errors are considered negligible in comparison to the injection errors and are ignored. At I + 5 days it is also assumed that a break in the pointing of the spacecraft high gain antenna from Earth lock is tolerable for several minutes with the communications maintained with an omni-antenna and the Pioneer is precessed to align its propulsion motor along the desired velocity correction direction. This is the only time during a mission in which the "full Pioneer precession" maneuver is permitted. All subsequent maneuvers employ the "restricted direction" maneuver wherein the velocity correction is applied as two sequential maneuver components, one component along the Earth vector and one component normal to the Earth line.

The I+5 day precession maneuver has resulting execution errors which map to the first planet B-plane miss errors. These errors are corrected by a second maneuver at 200 days before this planet's periapsis (E - 200). At E - 5 days, sufficient information about the orbit determination error at the E - 60 day epoch has been gained to make a third small correction to arrive at the nominal aim point at periapsis. The 60 days before encounter epoch is chosen since at this time sufficient radio tracking will have taken place such that orbit determination errors will be fairly representative of average errors along the entire tracking arc. Since this maneuver is quite small ($\approx$7 m/sec), the execution errors do not map in 5 days to significant errors at periapsis and are hence ignored.

For the SU and JU missions, there still remains a small orbit determination uncertainty at the intermediate planet's periapsis which is then mapped to a large uncertainty at Uranus encounter. Thus, a fourth velocity correction is performed at 50 days past the intermediate planet's periapsis (E+50) to correct for these Uranus errors. The execution errors from this maneuver are mapped to Uranus B-plane errors. A further velocity correction is made to correct these errors and the resulting execution errors mapped to Uranus B-plane errors ar. considered acceptable to the mission objectives of probe release and entry. At Uranus minus 120 days (U - 120) the approach phase radio begins and at U - 24 days meaningful optical measurements can be taken to establish the spacecraft orbit with respect to Uranus before the bus is deflected from the planetary-aimed probe. Actually, a small velocity correction to the bus/probe would be made before bus separation to correct the orbit determination errors. The resulting execution errors of the bus are then mapped to various epochs prior to and including probe atmospheric entry. The bus errors are then mapped to bus periapsis as well. The mapping

of the errors permits analysis of the entry condition errors which are important to the communications, structural and science designs for the probe.

Table 3 summarizes the multi-planet maneuver sequences after Ref. 4.

Analysis

Reference 5 documents in detail the mathematical derivations and analyses performed in supporting the navigation and guidance results presented below. In the limited space here, it suffices to state that observable clock and cone angles of V-slit satellite and star measurements are related geometrically to the spacecraft state vector, satellite orbital elements, and the spacecraft spin axis orientation. Using the dynamics relating spacecraft states at various times, a spacecraft covariance matrix at closest approach to a planet can be computed by a recursive filtering approach equivalent to that obtained by a linearized Kalman-type filter.

Midcourse velocity corrections are statistically derived by sampling various velocity covariance matrices at maneuver epochs by Monte Carlo sampling techniques. Drawn velocity vector samples from maneuver 1 are processed by the standard Pioneer precession model software (ref. 6) whereas subsequent epoch maneuver samples are processed by the restricted direction model (ref. 5) to obtain average execution errors which are in turn mapped to B-plane dispersion ellipses. The restricted direction maneuver, at long distances from Earth, avoids precessing of the spin axis and the subsequent temporary loss of Earth communications due to the redirecting of the Pioneer high-gain antenna.

Results

Navigation

1. Direct Saturn Mission. Unless specifically stated to the contrary, all subsequent navigation and maneuver B-plane errors correspond to bus or probe encounter (periapsis). Figure 3 displays the B-plane semi-major axis for the bus/probe as a function of data arc for the case of conventional plus differenced radio navigation. Here, unlike the conventional analysis, the results are monotonically decreasing. This is most satisfying in that it removes the implicit problem of "optimal data spans," which appears to plague conventional results. It should also be mentioned that these results are a significant improvement over the conventional data-only analysis, especially when tight station location errors are assumed. In this particular case, the longest (best) data arc yields errors of approximately 1500 km. This implies that the dominant factors in the state errors (using the longest data arc) are the ephemeris and mass errors of the planet. In other words, to significantly reduce the state error below 1500 km would require a more precise a priori knowledge of both the ephemeris and mass of Saturn.

2. Saturn/Uranus Mission. The Saturn and Uranus radio-only results are shown in Fig. 4 for both "tight" and "loose" station location error assumptions. The curves for Saturn indicate that the choice of the initial data epoch has but a slight effect on the estimation accuracy, as has the data termination time. The major effect upon estimation capability, however, is due to the assumed level of station location errors; the results using the "loose" assumption being roughly twice those of the "tight." Thus it appears that lengthy tracking intervals, or extension of tracking close to Saturn encounter, have little effec. in reducing estimation errors, whereas improvement in station location errors can have highly beneficial results.

It is obvious from the Uranus radio curves that the predominant source of error is the ephemeris. The addition of data near encounter does not affect the level of error at all. Even the change from "loose" to "tight" station location errors hardly improves the radio-only estimation capability when the spacecraft is in the presence of such enormous ephemeris errors.

For the optical measurements and filter at Saturn, initial estimates of 162,000 km for the spacecraft Z component and -959,000 km/day for $\dot{X}$ were assumed. The X axis is defined in the direction of the approach velocity vector - the XY plane is the approach orbital plane. All other spacecraft state components were taken as 0. Apriori standard deviations of 10^6 km in components of spacecraft position and 10^{-4} km/day in velocity components were assumed. An apriori satellite semimajor axis uncertainty of 10^6 km was assumed as well as 1 rad for satellite inclination i and right ascension of ascending node Ω. A V-slit sensor bias of 0.05 mrad was assumed. Random errors in the cone and clock angle observable are 0.08 and 0.12 mrad respectively. Figure 5 shows the B-plane semimajor axis as a function of the tracking arc for Saturn's satellites. Although Fig. 5 shows the results assuming 24 optical measurements per day with the sensor bias estimated, Ref. 5 parameterized the sample rate and "considered" bias, which result in the following conclusions:

1. Apparently, one complete orbit of data (independent of choice of satellite) is required to achieve navigation accuracies of less than 3000 km.

2. The ultimate accuracy that can be attained for a given data arc depends on the orbital period of the satellite. For the same span of time, it would be more desirable to view a satellite. such as Rhea, of shorter period rather than a longer-period satellite such as Titan.

3. Considering the bias yields errors that are about 25% greater than estimating the bias during the first few orbits of data. However, after several orbits of data, there is only about 4% difference between these cases.

4. The navigation accuracy apparently varies inversely with the square root of the sampling rate.

The optical navigation problem for Uranus is considerably different than that for Saturn, in terms of the number of orbits of data available and the viewing geometry. Only the satellites Ariel, Titania, and Oberon are examined for the Uranus approach. They have periods ranging from 13.4 to 2.5 days with the earliest acquisition occurring only 25 days before encounter. Since a probe is to be released no later than 14 days before encounter, this implies that a maximum of 11 days of data is available, regardless of which satellite is viewed.

The spacecraft motion was again assumed to be parallel to the X-Y plane, however, the satellite orbits are in the Y-Z plane. The initial spacecraft Z component was assumed as 130,000 km and the $\dot{X}$ component as -1.19×10^6 km/day; all other components taken as 0. All satellite inclinations i and right ascensions Ω were assumed to be $\pi/2$. A priori standard deviations of 30,000 km in position and 10^{-4} km/day in velocity were assumed for the spacecraft. For the satellites, 10,000 km in semimajor axis and 1 rad in i and Ω were assumed. The a priori errors of the spacecraft state are the result of processing radio data from 120 days to 26 days before encounter. The same sensor statistics and sampling rates are assumed for the baseline mission as were used for the Saturn study.

Figure 6 presents the optical tracking results for the Uranus approach. Reference 5 reveals that "considering" the bias yields B-plane errors that

are about three times larger than when estimating the bias. Figure 6 is the case when the spacecraft state, spin axis, and sensor bias are all estimated. The sample rate is 4 per day. When the bias is estimated, the error varies in the expected $1/\sqrt{N}$ manner (N being the sample rate). For the considered case, however, the errors are relatively insensitive to sampling rate. Increasing the sensor error by a factor of two results only in about a 10% increase in the estimation error.

The optical navigation accuracies for the Uranus approach are strongly affected by the relative viewing geometry. A major error source is the inability to accurately determine the nodal angle of the satellite orbit. For the Saturn approach geometry the error in the nodal estimate is about 0.48×10^{-2} rad, whereas for the Uranus case this error is about 0.2×10^{-1} rad. However, even when considering the effects of bias errors, navigation accuracies of less than 1500 km can be achieved as early as 19 days before encounter.

3. Jupiter/Uranus Mission. The Jupiter phase radio-only results are shown in Fig. 7 for both "tight" and "loose" station location error assumptions. Here, as in the Saturn phase of the Saturn/Uranus Mission study, these different assumptions yield results that vary by almost a factor of 2. Figure 7 also reveals the importance of data span. Significant improvements are attained by using longer arcs if data terminate around 20 days prior to encounter. If, however, data are taken to within 6 days of encounter, then the length of the arc is not very important. With the assumption of "tight" station location errors, B-plane errors at Jupiter of about 400 km appear achievable.

The B-plane errors for both the probe and the bus at Uranus as a function of data arc are identical to those shown in Fig. 4 for the Saturn/Uranus mission. Here, as in the Saturn/Uranus mission analysis, the

results are independent of data arc and the level of station location error. The major source of error in these results is, of course, the ephemeris and mass error of Uranus.

The assumptions employed in the optical navigation during Jupiter flyby are 5000 km spacecraft position component errors and 1 m/sec velocity component errors when tracking the Gallilean satellites and 3000 km and 0.1 m/sec when tracking Amalthea. The a priori error in semimajor axis for all Jupiter satellites is taken to be 30,000 km; a 1 rad error is assumed for i, Ω, and ϕ_0 (the argument of periapsis plus satellite true anomaly). A 0.1 rad error is alloted to α and δ for estimating the right ascension and declination of the spacecraft spin axis. The sensor clock and cone angle biases are again taken to be 0.05 mrad. The same error values are taken at Uranus except that spacecraft position component errors of 30,000 km and velocity component errors of 1 m/sec are assumed. Random cone and clock angle errors are again 0.08 and 0.12 mrad respectively.

Figure 8 presents the optical results for the Jupiter satellites tabulated in Table 2. Only the most optimistic cases are shown in which the spacecraft state, spin axis, and sensor bias are all estimated. All tracking cases are based on four measurement samples per day.

From Fig. 8 it may be concluded that the Gallilean satellites (Callisto, Ganymede, Europa, and Io) do not appear to be very good candidates for V-slit optical orbit determinations. Because of their size, data must terminate long before planetary encounter (at least with this particular sensor), and as a result insufficient state information is acquired. The satellite Amalthea presents a somewhat better situation in that it has a short

period and can be tracked virtually to encounter. The spread in the results between the various cases examined, however, is quite large, ranging at most from 230 to 1000 km in the most pessimistic case. The large size of the latter case is due to the brevity of the data span. If a longer tracking interval could be assumed, this error would significantly reduce.

As a result, it appears that V-slit sensor optical data in the Jupiter phase does not particularly enhance state estimation over radio data alone. If Amalthea could be tracked, which is somewhat questionable due to the proximity of a very bright Jupiter, it appears to be the only satellite examined which is capable, in the more optimistic cases, of providing better state estimates than radio data alone.

The results obtained by tracking Uranus satellites Oberon, Titania, and Ariel have been seen in Fig. 6. The trajectory approach conditions between the Saturn/Uranus and Jupiter/Uranus missions do not differ significantly enough to affect the optical navigation results after the filter has had adequate time to reduce the conservatively large a priori errors. Here, as shown in the Uranus phase of the SU mission, enormous gains in state estimation can be achieved by using radio and optical data instead of radio data alone.

B-plane errors on the order of 1000-1500 km appear easily achievable regardless of which satellite is tracked, when data can be taken to E-12^{d} (the candidate separation time nearest to encounter).

Optical navigation using the satellite Titania was also investigated with the sample rate varied for the case of estimating the states of the spacecraft, Titania, and spin axis orientation, and considering the bias. The B-plane error with the full data arc appears to reduce in the $1/\sqrt{N}$ manner as data sample rate is increased. As a result, fairly significant

improvement in the radio plus optical orbit determination accuracies for all satellites of Jupiter and Uranus can be effected if the concomitant penalty of a higher sampling rate is acceptable.

Maneuvers

Table 4 summarizes the velocity requirements for the three outer planet missions. The event numbers correspond to those of Table 3. For the direct Saturn mission note that the Monte Carlo sampling spread (variance) about the mean for the components can, and sometimes do, exceed the spread about the mean for the absolute value of the velocities. For the Saturn/Uranus mission, the first value of each pair at velocity correction numbers 4 and 5 pertains to radio-only navigation at Saturn while the second value pertains to the optical V-slit sensor. For the Jupiter/Uranus mission, the triplet at velocity correction numbers 4 and 5 correspond in order to radio "loose," radio "tight," and optical "Amalthea" tracking at Jupiter. The velocity deflection maneuvers 6 are taken as the maxima occurring at 700 and 600 Uranus radii respectively for the S/U and J/U missions.

It is interesting to note that all three missions have similar velocity requirements on the first leg-from Earth to the first encounter planet. The direct Saturn mission has a significantly less first velocity correction of 75 m/sec compared to 80 m/sec for the multi-planet missions. The higher S/U and J/U corrections than the direct Saturn correction are due to the intermediate planet aiming constraints for successful Uranus encounter. The second velocity correction for the Saturn/Uranus mission is three times greater than the corresponding Jupiter/Uranus correction. This is due to the correspondingly greater propagation time of the first maneuver execution errors of the S/U mission over the J/U mission.

The execution errors of this second velocity correction (13.6, 14.0, 4.6 m/sec for the S, S/U, and J/U missions respectively) map to one-sigma B-plane dispersion ellipses shown in Figures 9, 10 and 11. Note that, except for the large 2500-km miss at Uranus for the radio "loose" tracking about Saturn, all B-plane semimajor axes for the mapped second maneuver execution errors are in the range from 150 to 1000 km, well below the a priori spacecraft state vector errors assumed for the encounter navigation filter. This maneuver error domination by the a priori navigation errors is the factor which permits the navigation filter and the interplanetary maneuver statistics to be separated in this analysis.

The dispersion ellipses at the first encounter planets are aligned roughly in the ecliptic plane, whereas out-of-plane navigation errors during first planet flyby navigation orient the Uranus ellipses essentially normal to the ecliptic. The one exception to this trend is Amalthea optical tracking at Jupiter (Fig. 11) — the nearness of Amalthea to its primary apparently reduces the out-of-plane effect and the Uranus B-plane ellipse is reoriented to the ecliptic.

Table 4 reveals the advantage of optical tracking for multi-planet missions involving Saturn as the first encounter planet. Optical tracking improves the ephemeris and mass knowledge of Saturn; the corresponding improvement in spacecraft navigation near Saturn reduces the post encounter velocity correction by a factor of 6, from 139.3 m/sec for radio-only to 23.2 m/sec for radio plus optical. Note for Jupiter, whose mass and ephemeris are fairly well known, there is no improvement with the optical V-slit sensor; as a matter of fact, the optical measurements are sufficiently crude relative to radio tracking and planetary knowledge that they actually degrade the filter. Thus radio tracking-only with an assumed "loose"

station configuration requires a post-Jupiter correction (13.4 m/sec) or 6 m/sec less than that required using optical coupled with radio (19.2 m/sec).

Table 4 also reveals the significant velocity correction (7 and 9.8 m/sec for the S/U and J/U missions respectively) necessary to retarget the spacecraft to the nominal B-plane aim-point after sufficient orbit determination knowledge is learned during the first planet approach. This correction is necessary to insure nominal encounter at the next planet.

Conclusions

The radio navigation analyzed in the Saturn mission supports the following two conclusions: (1) The addition of differenced data to conventional data dramatically improves state estimation capability, from 3000 to 1500 km assuming "tight" stations for the Saturn mission. This improvement is such, in the case of "tight" station locations, that for further gains to be made, significant reductions in the level of the a priori errors in the ephemeris and mass of Saturn must be effected. (2) Proper weighting of the available data types must be made, in the presence of stochastic accelerations, so as to extract the maximum amount of state information the data types contain.

A total propulsion capability of 200 m/sec would suffice for mid-course and separation velocity requirements for the direct Saturn mission.

In the Saturn approach phase of the Saturn/Uranus mission, radio data alone appear able to meet certain mission constraints (B-plane semimajor axis errors of 1000 km or less) if "tight" station location errors are provided. When optical data are coupled with radio data, however, navigation accuracies for the Saturn approach phase on the order of 200 km can be attained using one of several candidate satellites of Saturn. The main

argument for the inclusion of optical data is the factor of six savings in the Saturn-Uranus leg velocity requirements – from 140 m/sec with radio "loose" to 23.2 m/sec for radio coupled with optical V-slit measurements. The radio-only navigation accuracy in the Uranus phase is completely limited by the ephemeris errors of the planet, which are on the order of 10,000 km. Incorporating optical data at Uranus can provide navigation errors of 1500 km for tracking up to 1000 Uranus radii (R_U) (or encounter E - 20 days) or 1000 km for tracking up to 700 R_U (E - 14 days).

For the Jupiter phase of the Jupiter/Uranus mission, radio-only state information can yield B-plane errors on the order of 400 to 800 km, depending on the level of station location error that is appropriate. The Uranus phase radio-only errors are equivalent to those of the Saturn/Uranus mission. The coupling of radio with optical data in the Jupiter phase does not appear to significantly enhance orbit determination capability without resorting to fairly high optical sampling rates. For a higher sampling rate, satellite Europa appears to be a good candidate with which to obtain reduced state errors. If the assumptions about the optical instrument are truly valid, namely that assumed biases in cone and clock angles are actually biases (not slowly drifting or oscillating parameters) and hence can be adequately and properly included in the estimation, then satellite Amalthea appears to provide excellent orbit errors (if of course it can be seen in such near proximity to Jupiter) on the order of 220 to 350 km (these, however, are with a data arc extending to within one day of encounter). In the Uranus phase optical data, in addition to radio, significantly reduce state errors to the level of 1000 to 1500 km.

The direct Saturn mission is navigationally feasible using Earth-based tracking. This mode of navigation suffices for the Jupiter flyby portion of the Jupiter/Uranus mission if a reasonable propellant load is carried (<225 m/sec including separation maneuver). An on-board optical system with the characteristics and accuracy of the V-slit sensor is necessary for probe entry into the atmosphere of Uranus on both the Saturn/Uranus and Jupiter/Uranus missions. The optical sensor is also highly desirable during the Saturn encounter of the former mission in the sense that a propellant savings of roughly 132 m/sec can be effected thereby on the Saturn-Uranus leg.

Acknowledgments

The authors would like to acknowledge the helpful suggestions regarding this research by Dr. Louis D. Friedman, Robert T. Mitchell, and Raymond B. Frauenholz of the Jet Propulsion Laboratory. The work reported herein is part of a study led by the NASA-Ames Research Center. The cooperation of Messrs. Howard Mathews and Larry Manning of ARC, as well as Dr. William Dixon of TRW, is gratefully appreciated.

References

1. Swenson, B.L., Tindle, E.L., and Manning, L.A., "Mission Planning for Pioneer Saturn/Uranus Atmospheric Probe Missions," NASA TM-X-2824, Ames Research Center, Sept., 1973.

2. Ondrasik, V.J., Rourke, K.H., "Application of New Radio Tracking Data Types to Critical Spacecraft Navigation Problems," JPL Quarterly Technical Review, Vol. 1, No. 4, January 1972.

3. Duxbury, T.C., "A Spacecraft-Based Navigation Instrument for Outer Planet Missions," Journal of Spacecraft and Rockets, Vol. 7, No. 8, Aug. 1970.

4. Friedman, L.D., Hamilton, T.W., and Stanton, R.H., "Estimating Trajectory Correction Requirements for the Outer Planets Grand Tour Missions," AIAA Paper No. 72-54, AIAA 10th Aerospace Sciences Meeting, San Diego, Cal., Jan. 17-19, 1972.

5. Paul, C.K., Russell, R.K., and Ellis, J., "Advanced Pioneer Planetary Probe Mission Guidance and Navigation Requirements," Jet Propulsion Laboratory Report 760-88, Pasadena, Cal., Nov. 15, 1973.

6. Frauenholz, R.B., "Project Document Pioneer F Jupiter Flyby 1972 Maneuver Analysis," Parts I and II, Jet Propulsion Laboratory Report 616-15, Sept. 1, 1971.

Table 1. Mission Trajectories

Trajectory Element / Mission	Earth Departure			Saturn Approach		Jupiter Approach	Uranus Approach	
	S	S/U	J/U	S	S/U	J/U	S/U	J/U
Date	11/23/79	11/25/80	12/9/80	4/16/83	1/5/84	3/25/82	11/9/87	4/2/86
velocity V_∞ (km/sec)	11.59	11.98	11.38	9.1	10.54	15.08	13.77	15.75
RA	138.74	170.5	170.1	180.3	193.2	57.1	25.0	111.3
δ	18.09	26.9	11.1	-2.3	-8.6	2.2	-67.8	-81.2
ϑ_{aim} (°)				-22	-28.7	0.81	-64.2	-145.2
r_p				2.6	2.73	14.67	4.0	3.0
γ_e				-30			-40	-40
B				3.4968			1.472	1.281

Separation Elements Considered	Missions							
	S (1)	S/U (3)			J/U (4)			
R	300	700	1000	1300	600	800	1000	1200
T	506.54	329.6	471.5	613.2	282.85	377.79	472.75	567.74
ΔV (along)	104	44.6	30.2	18.0	57	43	34	28
ΔV (normal)	0	65.8	46.2	36.2	60	45	36	30

Table 2. Satellites of Jupiter, Saturn, and Uranus

Satellite	Period (days)	Acquisition	Termination	Acquisition distance (km)
		JUPITER		
Callisto	16.689	J-62^d	J-35^d	3.6×10^8
Ganymede	7.155	J-420^d	J-39^d	5.5×10^8
Europa	3.551	J-313^d	J-23^d	4.2×10^8
Io	1.769	J-374^d	J-28^d	5.0×10^8
Amalthea	0.498	J-10^d	J-1^d	8.5×10^6
		SATURN		
Titan	15.9	S-150^d	S-49^d	15.0×10^7
Rhea	4.5	S-82^d	S-14^d	8.0×10^7
Dione	2.7	S-52^d	S-10^d	6.4×10^7
Tethys	1.9	S-52^d	S-16^d	6.5×10^7
Enceladus	1.37	S-40^d	S-5^d	3.8×10^7
Mimas	0.94	S-30^d	S-5^d	3.0×10^7
		URANUS		
Oberon	13.5	U-23.5^d	U-7^d	2.8×10^7
Titania	8.7	U-25.0^d	U-8^d	3.0×10^7
Ariel	2.5	U-23.5^d	U-5^d	2.8×10^7

Table 3. Multi-Planet Mission

Event Point	Description	Epoch
1	Earth launch	I + 0 days
2	1st velocity correction	I + 5 days
3	2nd velocity correction	J,S - 200 days
4	3rd velocity correction	J,S - 5 days
5	Jupiter, Saturn periapsis	J,S + 0 days
6	4th velocity correction	J,S + 50 days
7	5th velocity correction	U - 200 days
8	Bus separation maneuver	U - 13.7, 19.6, 25.6 days (SU)
		U - 11.8, 15.7, 19.9, 23.6 days (JU)
9	Uranus periapsis	U + 0 days

Table 4. Midcourse Velocity Requirements

Event	Velocity Correction Number	Saturn			Saturn/Uranus			Jupiter/Uranus		
		M[a]	A[b]	N[c]	M	A	N	M	A	N
2	1	74.7	31.1	74.1	80.1	29.2	79.6	79.3	30.6	78.9
3	2	13.6	14.1	8.6	14.0	12.0	10.7	4.6	2.5	4.3
4	3	104	104	0	7.0	6.4	4.5	9.8	5.3	9.2
6	4				(139.3, 23.2)	(38.6, 11.4)	(138.9, 22.4)	(13.4, 7.9, 19.2)	(2.8, 2.2, 13.2)	(13.2, 7.7, 16.2)
7	5				(18.7, 2.9)	(3.9, 0.9)	(18.7, 2.8)	(1.8, 1.1, 2.2)	(0.8, 0.6, 1.8)	(1.8, 1.0, 1.6)
8	6				110.4	44.6	65.8	117	57	60

a. M is mean plus three-sigma velocity magnitude in m/sec

b. A is the along-Earth-line mean plus three-sigma velocity component in m/sec

c. N is the normal-to-Earth-line mean plus three-sigma velocity component in m/sec.

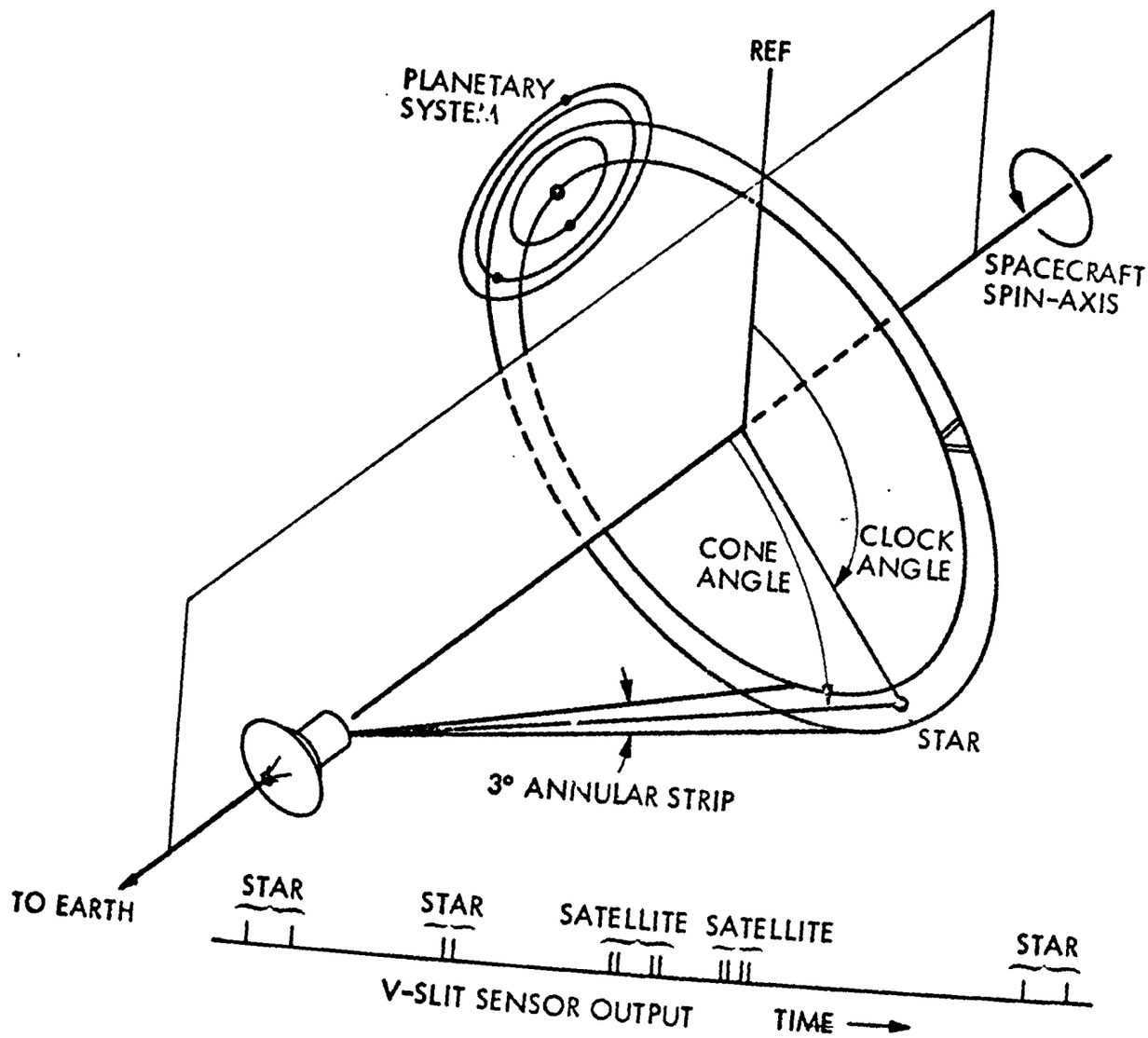

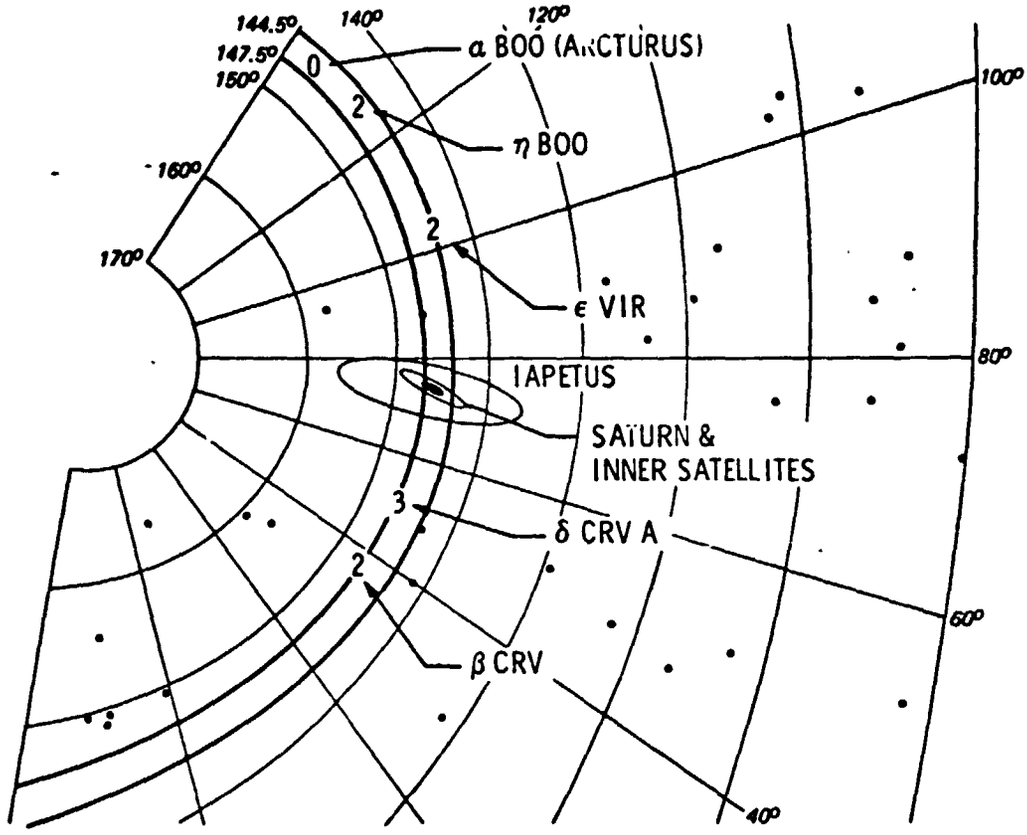

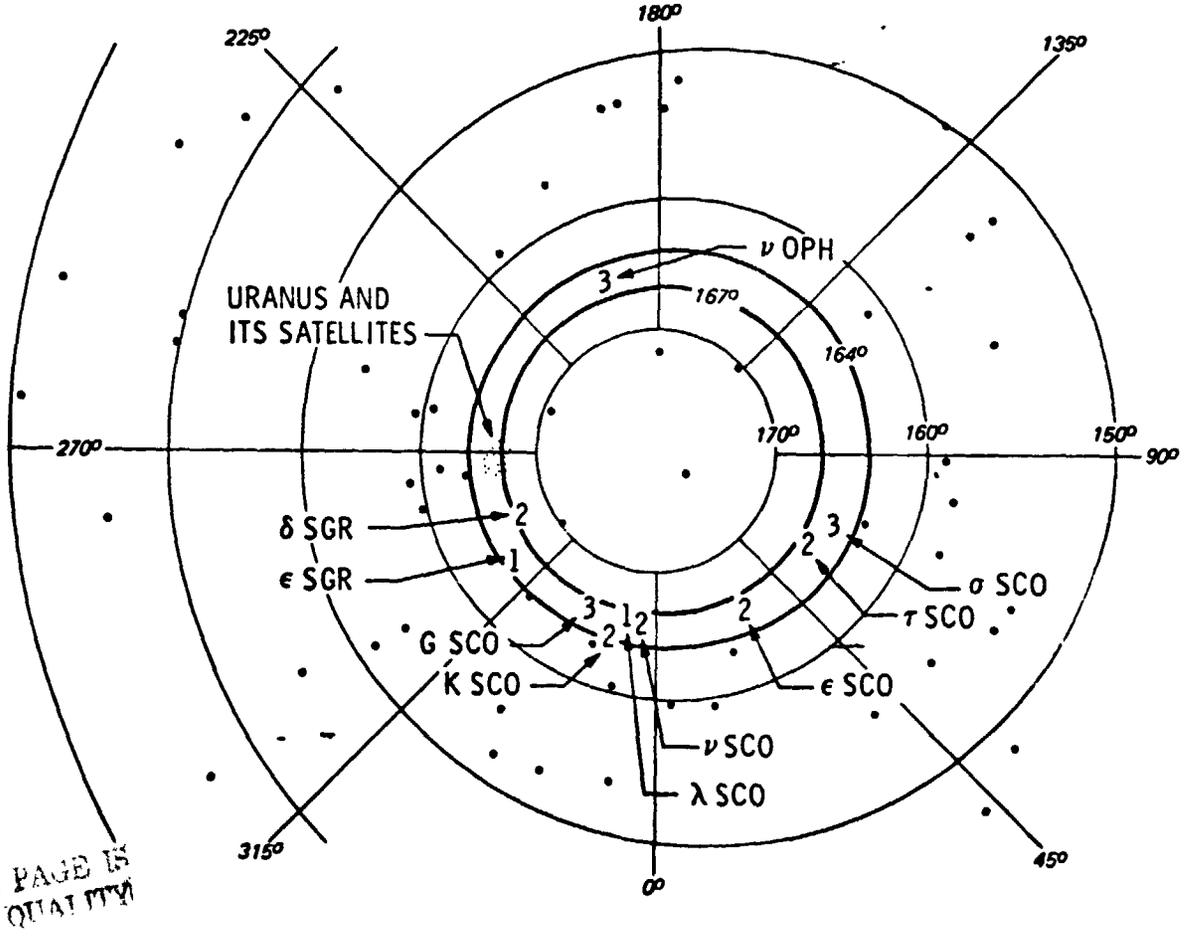

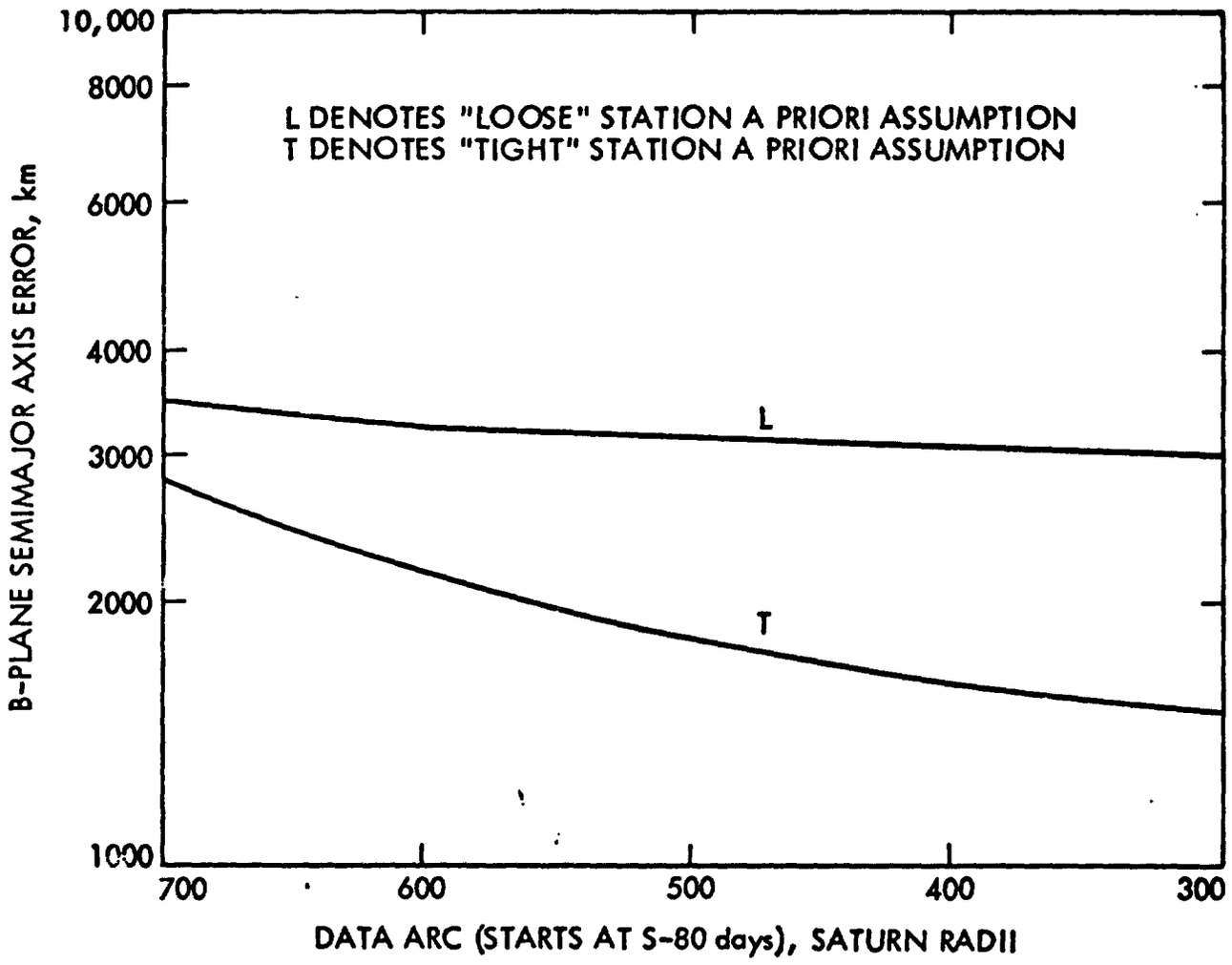
L DENOTES "LOOSE" STATION A PRIORI ASSUMPTION
T DENOTES "TIGHT" STATION A PRIORI ASSUMPTION
B-PLANE SEMIMAJOR AXIS ERROR, km
10,000
8000
6000
4000
3000
2000
1000
L
T
700
600
500
400
300
DATA ARC (STARTS AT S-80 days), SATURN RADII

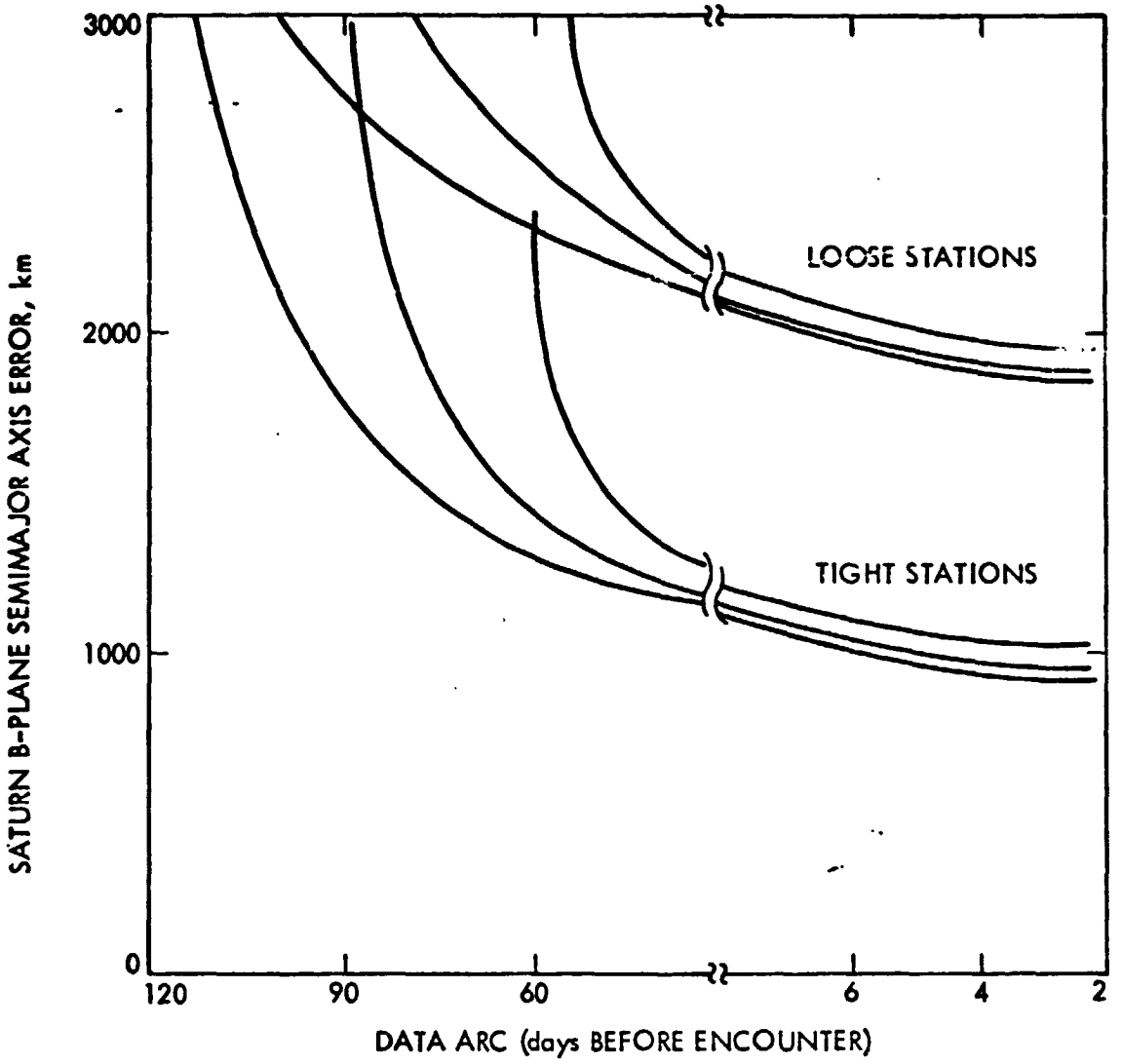
3000
2000
1000
0
SATURN B-PLANE SEMIMAJOR AXIS ERROR, km
LOOSE STATIONS
TIGHT STATIONS
120
90
60
6
4
2
DATA ARC (days BEFORE ENCOUNTER)

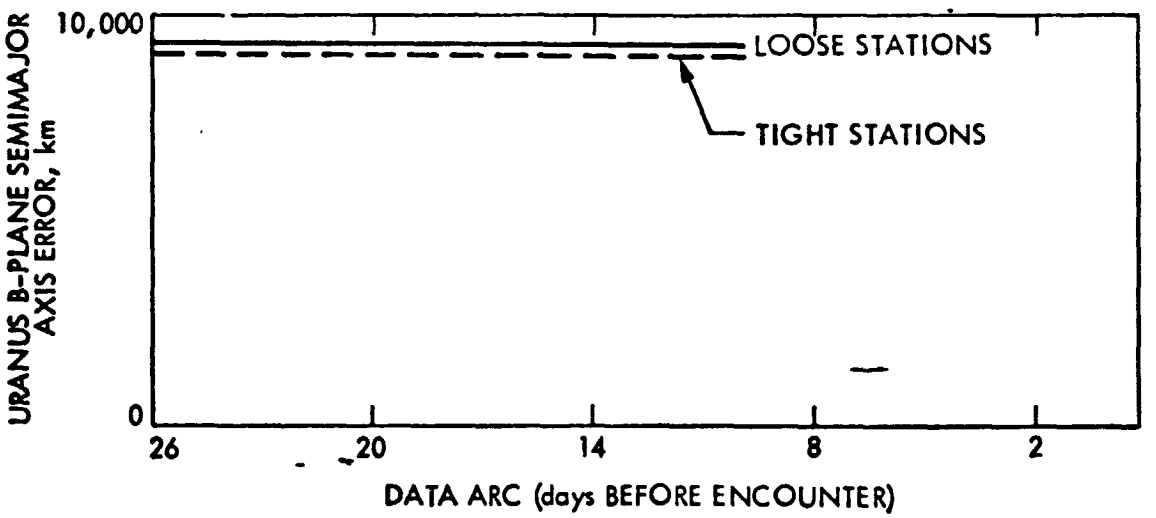
10,000
0
URANUS B-PLANE SEMIMAJOR AXIS ERROR, km
LOOSE STATIONS
TIGHT STATIONS
26
20
14
8
2
DATA ARC (days BEFORE ENCOUNTER)

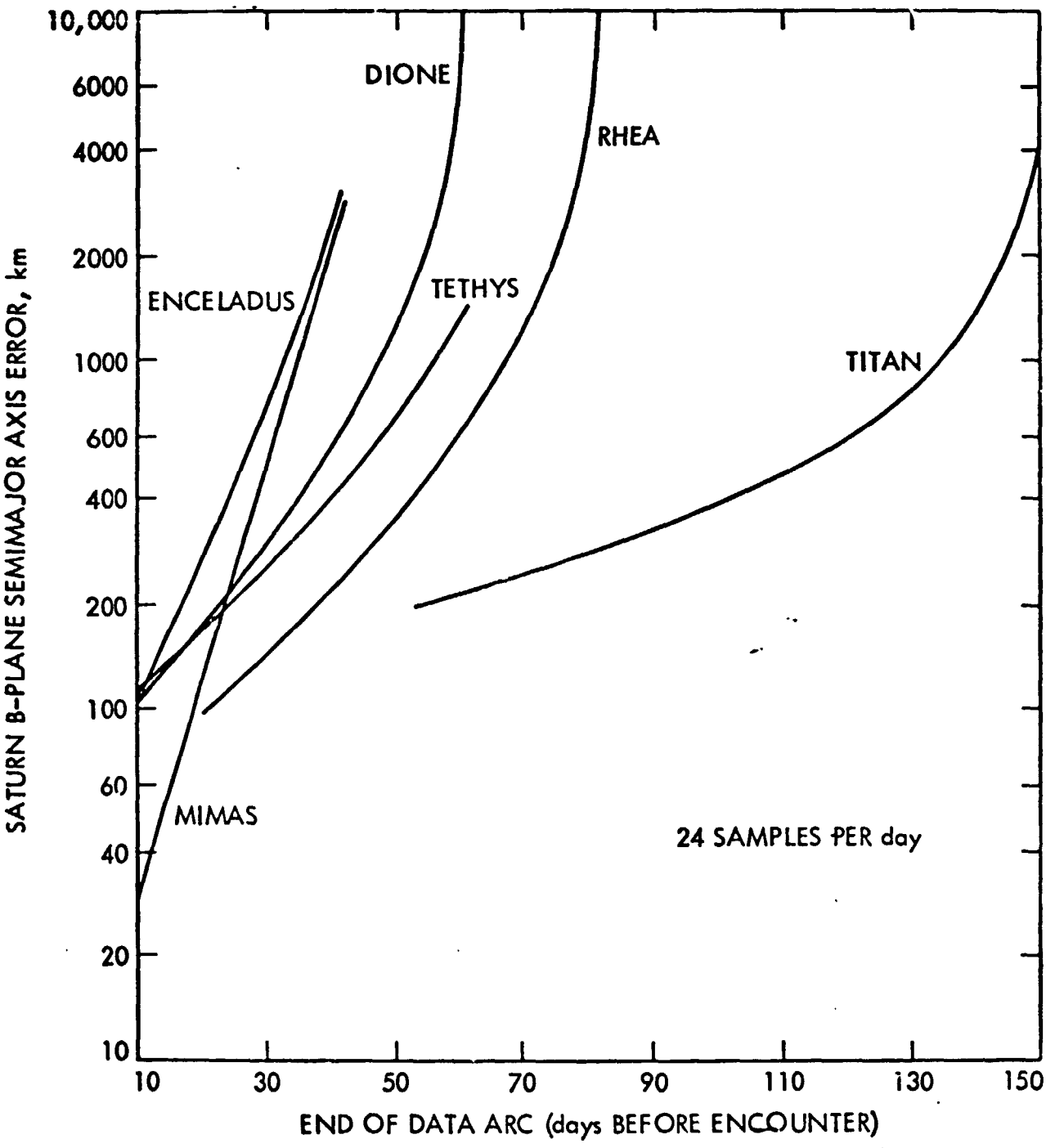
10,000
6000
4000
2000
1000
600
400
200
100
60
40
20
10
SATURN B-PLANE SEMIMAJOR AXIS ERROR, km
DIONE
RHEA
ENCELADUS
TETHYS
TITAN
MIMAS
24 SAMPLES PER day
10
30
50
70
90
110
130
150
END OF DATA ARC (days BEFORE ENCOUNTER)

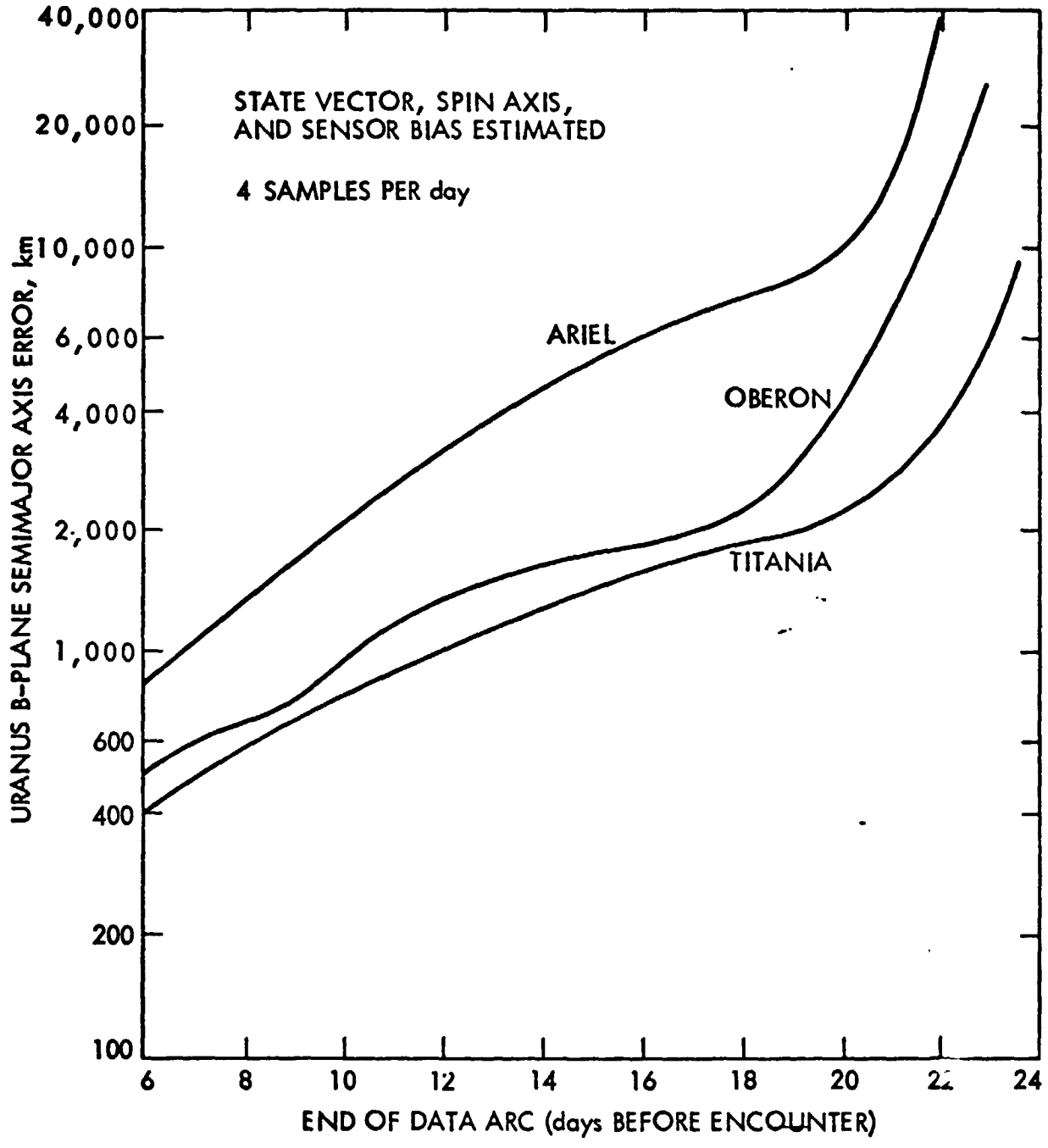
STATE VECTOR, SPIN AXIS,
AND SENSOR BIAS ESTIMATED
4 SAMPLES PER day
ARIEL
OBERON
TITANIA
URANUS B-PLANE SEMIMAJOR AXIS ERROR, km
40,000
20,000
10,000
6,000
4,000
2,000
1,000
600
400
200
100
6
8
10
12
14
16
18
20
22
24
END OF DATA ARC (days BEFORE ENCOUNTER)

F6

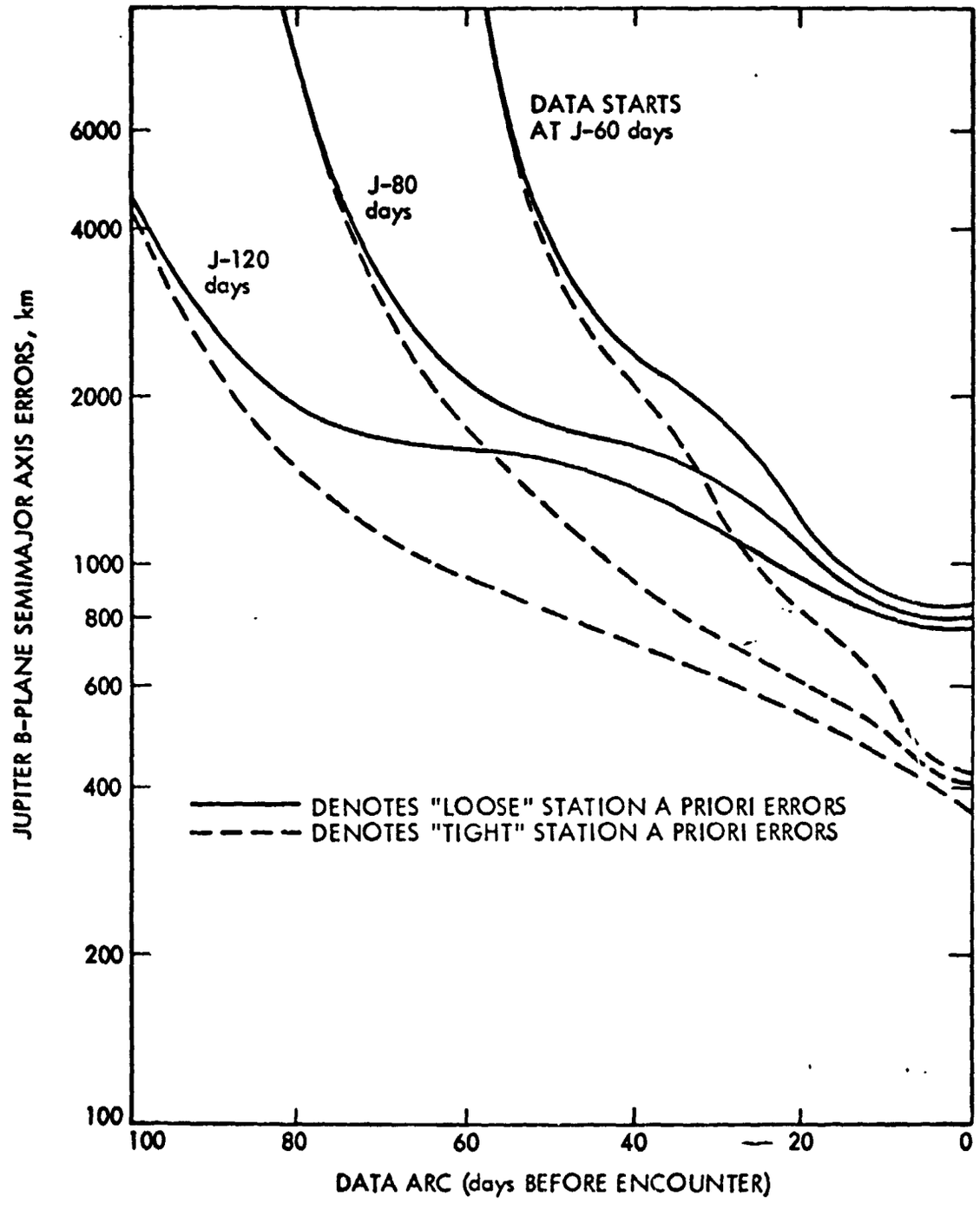
DATA STARTS
AT J-60 days
J-80
days
J-120
days
6000
4000
2000
1000
800
600
400
200
100
JUPITER B-PLANE SEMIMAJOR AXIS ERRORS, km
DENOTES "LOOSE" STATION A PRIORI ERRORS
DENOTES "TIGHT" STATION A PRIORI ERRORS
100
80
60
40
20
0
DATA ARC (days BEFORE ENCOUNTER)

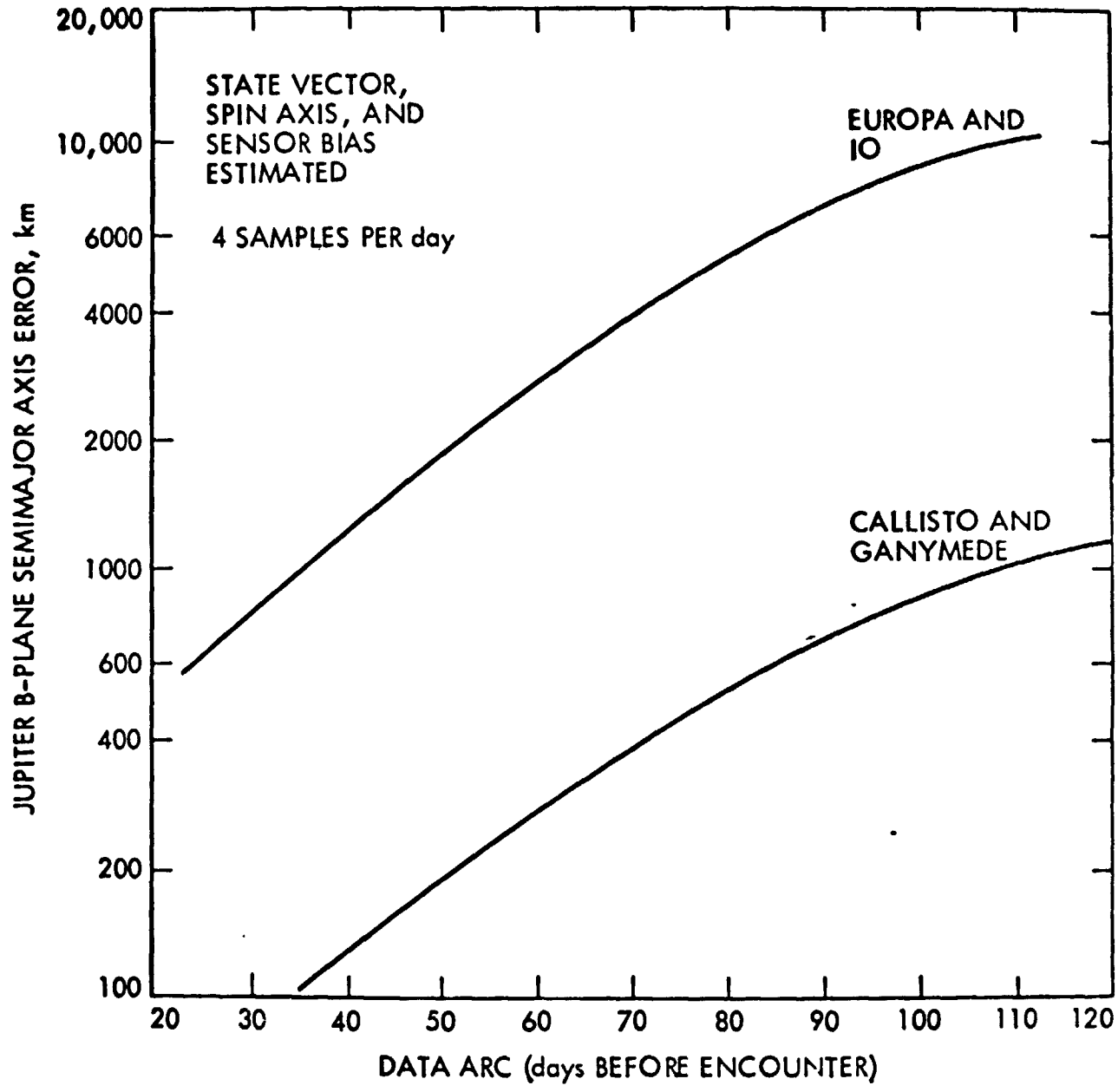
20,000
10,000
6000
4000
2000
1000
600
400
200
100
STATE VECTOR,
SPIN AXIS, AND
SENSOR BIAS
ESTIMATED
4 SAMPLES PER day
EUROPA AND
IO
CALLISTO AND
GANYMEDE
JUPITER B-PLANE SEMIMAJOR AXIS ERROR, km
20
30
40
50
60
70
80
90
100
110
120
DATA ARC (days BEFORE ENCOUNTER)

SEMIMAJOR AXIS: 1037 km
SEMIMINOR AXIS: 322 km
ORIENTATION ANGLE: 12°

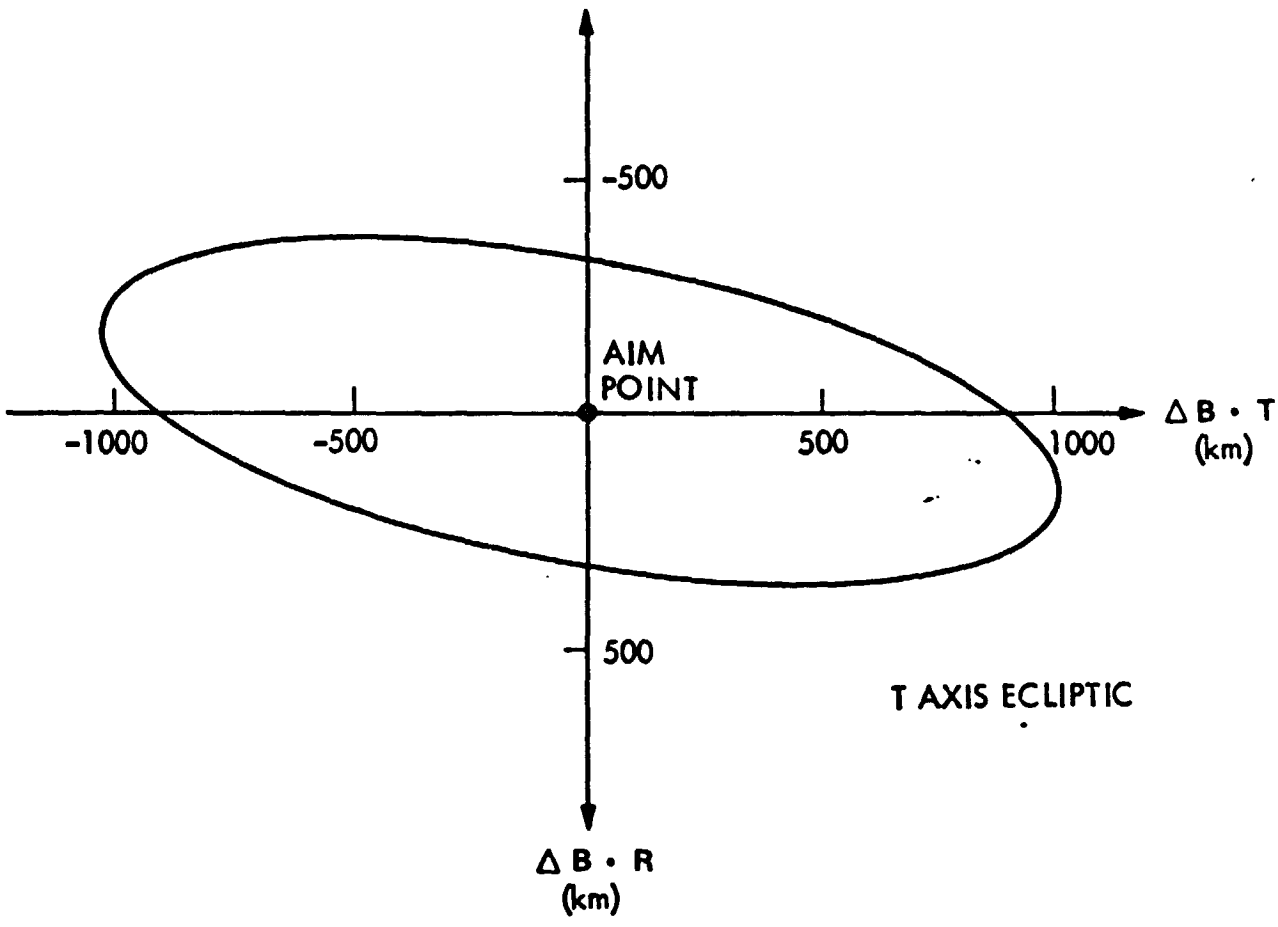

ERROR SOURCE: 2nd MANEUVER EXECUTION ERRORS

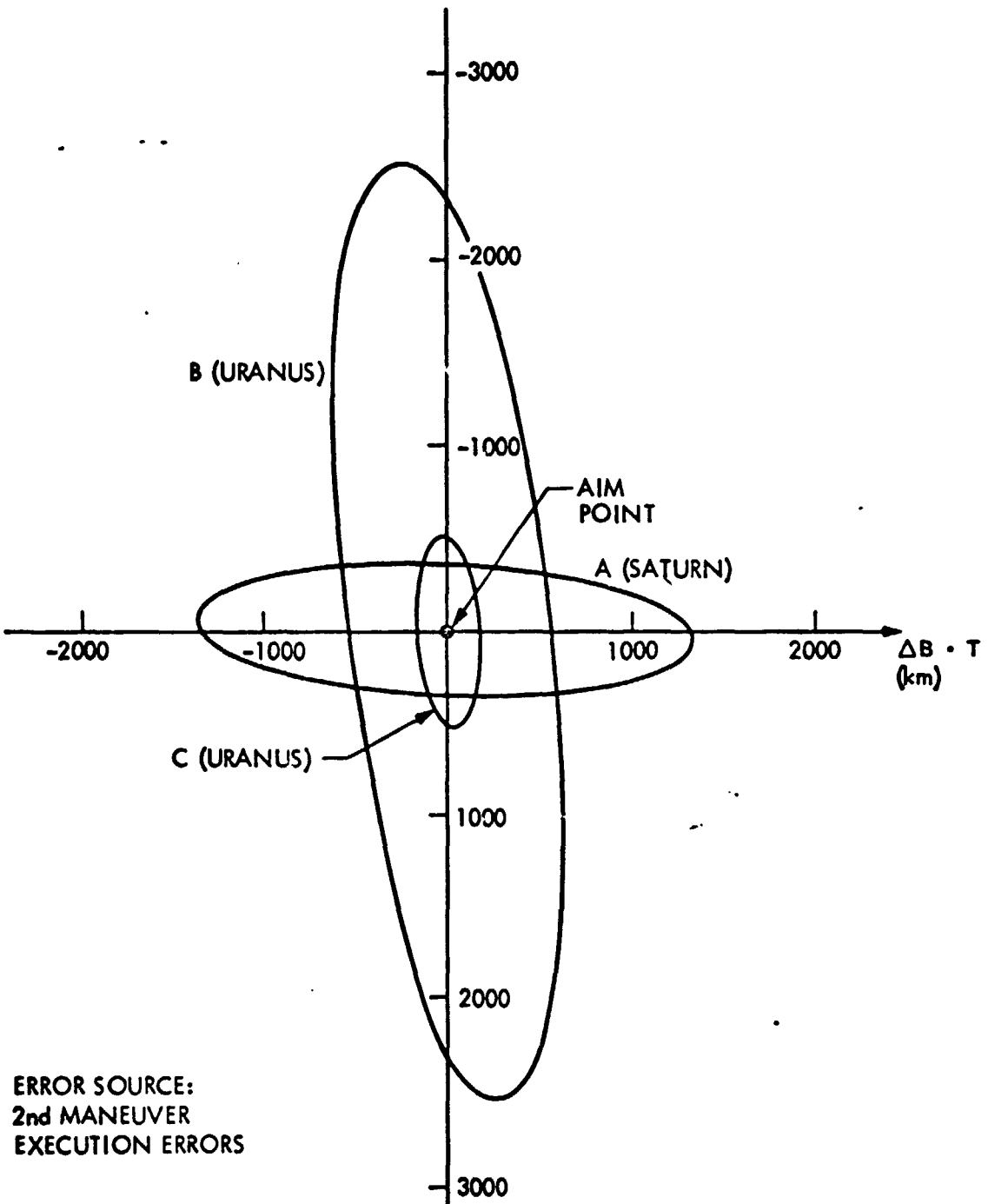

ERROR SOURCE:
2nd MANEUVER
EXECUTION ERRORS

σ_1: SEMIMAJOR AXIS (km)
σ_2: SEMIMINOR AXIS (km)
θ : ORIENTATION ANGLE (deg)

ELLIPSE	LEG	- DESCR	σ_1	σ_2	θ
A	ES	- RADIO	1373	350	2
B	SU	- RADIO	2551	551	84
C	SU	- OPTICAL	410	134	85

σ_1: SEMIMAJOR AXIS (km)
σ_2: SEMIMINOR AXIS (km)
θ : ORIENTATION ANGLE (deg)

ELLIPSE	LEG - DESCR	σ_1	σ_2	θ
A	ES - RADIO	554	302	7
B	JU - RAD-LOOSE	241	89	80
C	JU - RAD-TIGHT	133	70	82
D	JU - OPTICAL	216	68	177

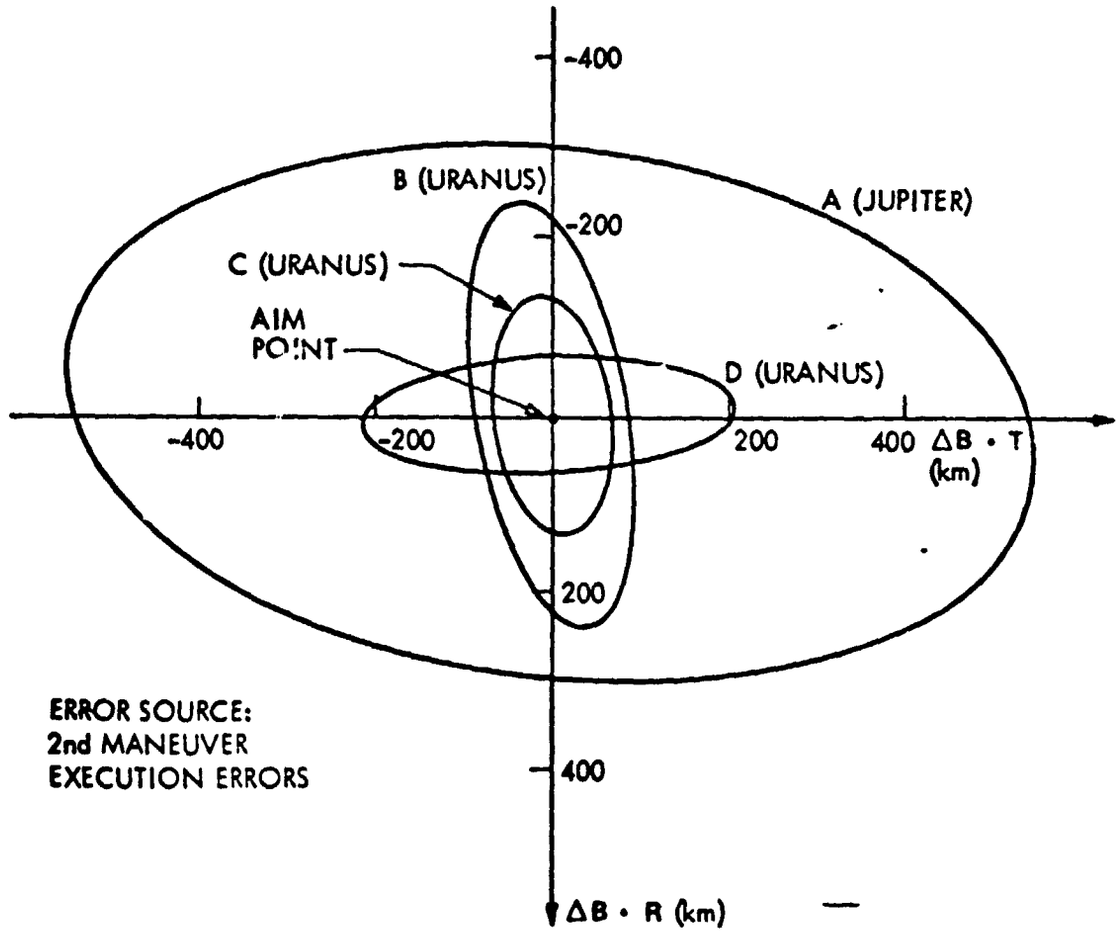

ERROR SOURCE:
2nd MANEUVER
EXECUTION ERRORS